Thermal transport in graphene and effects of vacancy defects

Hengji Zhang,[1] Geunsik Lee,[2] and Kyeongjae Cho[1,2,*]

[1]*Department of Physics, University of Texas at Dallas, Richardson, Texas 75080, USA*

[2]*Department of Materials Science and Engineering, University of Texas at Dallas, Richardson, Texas 75080, USA*

(Received 26 April 2011; revised manuscript received 20 July 2011; published 27 September 2011)

We have performed molecular dynamics simulations to investigate phonon transport in graphene at 300 K with the Green-Kubo method. We show that the thermal conductivity (TC) of pristine graphene is 2903 ± 93 W/mK, and the out-of-plane phonon mode contribution is 1202 ± 32 W/mK. We further investigate thermal transport in graphene with different vacancy defect concentrations, and the TC shows that it is possible to achieve a maximum of a thousandfold reduction with a high defect density.

DOI: 10.1103/PhysRevB.84.115460 PACS number(s): 65.40.−b, 63.20.D−, 66.70.−f, 65.80.Ck

I. INTRODUCTION

In the past few years, extensive research on heat transport in graphene from experiments,[1–3] theories,[4,5] and simulations[6,7] has demonstrated an ultrahigh thermal conductivity (TC), which is crucially important for diverse applications, such as thermal management in electronics[8] and thermal conductance enhancement for composite materials.[9] The TC of isolated pristine graphene calculated with the Boltzmann transport equation (BTE)[4,5] has shown good agreement with experiments (a value between 2000 and 3000 W/mK).[1,2] However, a defect-free structure is not a practical assumption in that graphene would inevitably contain single-vacancy defects, as observed in experiments.[10] The vacancy defect in graphene can be introduced by the chemical synthesis method. The chemical reduction of graphene oxide, for example, provides us with a feasible way to synthesize graphene on a large scale, meanwhile, the apparent D peak from the Raman spectrum of completely reduced graphene oxide indicates that a large number of vacancy defects may exist in graphene.[11] Therefore, quantitatively examining the impact of vacancy defects on heat transport in graphene would not only reveals unique features that are difficult to probe by experiment on a nanoscale, but also suggests a general guidance on tuning the TC of graphene to a higher or lower value.

In this paper, we use a recently optimized reactive empirical bond-order (REBO) carbon potential[12] for running molecular dynamics (MD) simulations, and calculate the TC of graphene at 300 K with the Green-Kubo method.[7,13] We show that, for isolated pristine graphene, our simulation result (2903 ± 93 W/mK) is consistent with BTE theories[4,5] and experiments.[1,2] In addition, we find that ∼43% of phonon heat energy is transferred via out-of-plane modes [i.e., mainly from acoustic flexure modes (ZA)], and our result addresses a previous controversy in BTE theories[4,5] on whether a small group velocity of long-wavelength ZA modes can lead to a negligible heat transport contribution. Afterward, we primarily investigate the TC of graphene as a function of vacancy-defect concentration. In the case of vacancy defects, a rapid ∼25-fold reduction of TC is observed for graphene with 0.42% randomly generated vacancies, and it can be further decreased to 3.08 ± 0.31 W/mK (∼940-fold reduction) when the vacancy concentration reaches 8.75%. Such a high vacancy concentration might be possible for graphene synthesized through the chemical reduction of graphene oxide,[11] and an even higher vacancy concentration might be possible for graphene oxide with ∼30% mass loss after thermal exfoliation.[14] We also analyzed the phonon density of states (DOS) of graphene with vacancy defects, from which we observed broadening of the phonon mode peaks and average increase of DOS for low-frequency modes. Both of these factors can help to understand the abrupt TC reduction as the vacancy defects increase. Our simulations demonstrate that phonon transport in graphene can be strongly influenced by its vacancy defect concentration.

II. THEORY AND SIMULATION METHODS

A. MD simulation potentials

Among a few important factors in phonon transport simulation, the interatomic potential is one that fundamentally dictates the accuracy of TC. According to previous studies, the original REBO potential tends to underestimate the TC of carbon nanotubes[12,15] and graphene,[7,12] while the Tersoff potential tends to overestimate it.[6,12] Although a quantitative discrepancy exists between the results from simulations and experiments, a previous simulation modeling indeed promotes our understanding of the nature of phonon transport in low-dimensional carbon materials.[16] Here, for the sake of better accuracy, we use an optimized REBO carbon potential.[12]

In Figs. 1(b) and 1(c), we show a comparison of the phonon dispersions of graphene among the results from density function theory (DFT),[17,18] the original REBO,[19] and the optimized REBO.[12] One important feature with the optimized REBO is that it can exactly reproduce DFT phonon dispersions of three acoustic modes near the Brillouin zone center, i.e., LA, TA, and ZA. This suggests that the optimized REBO gives a more accurate prediction for the group velocity of long-wavelength acoustic modes,[12] which are mainly responsible for ultrahigh TC of graphene.[4,5] Even though optical modes are overestimated, it is very unlikely for those modes to be exited at room temperature, and should have less influence on the TC of graphene. Such an improvement on TC calculation has been confirmed in the BTE approach.[5,12] Hence, we expect that using this optimized potential in MD simulations should not only preserve the accuracy observed in the BTE work,[5,12] but also circumvent issues of using the BTE as it cannot

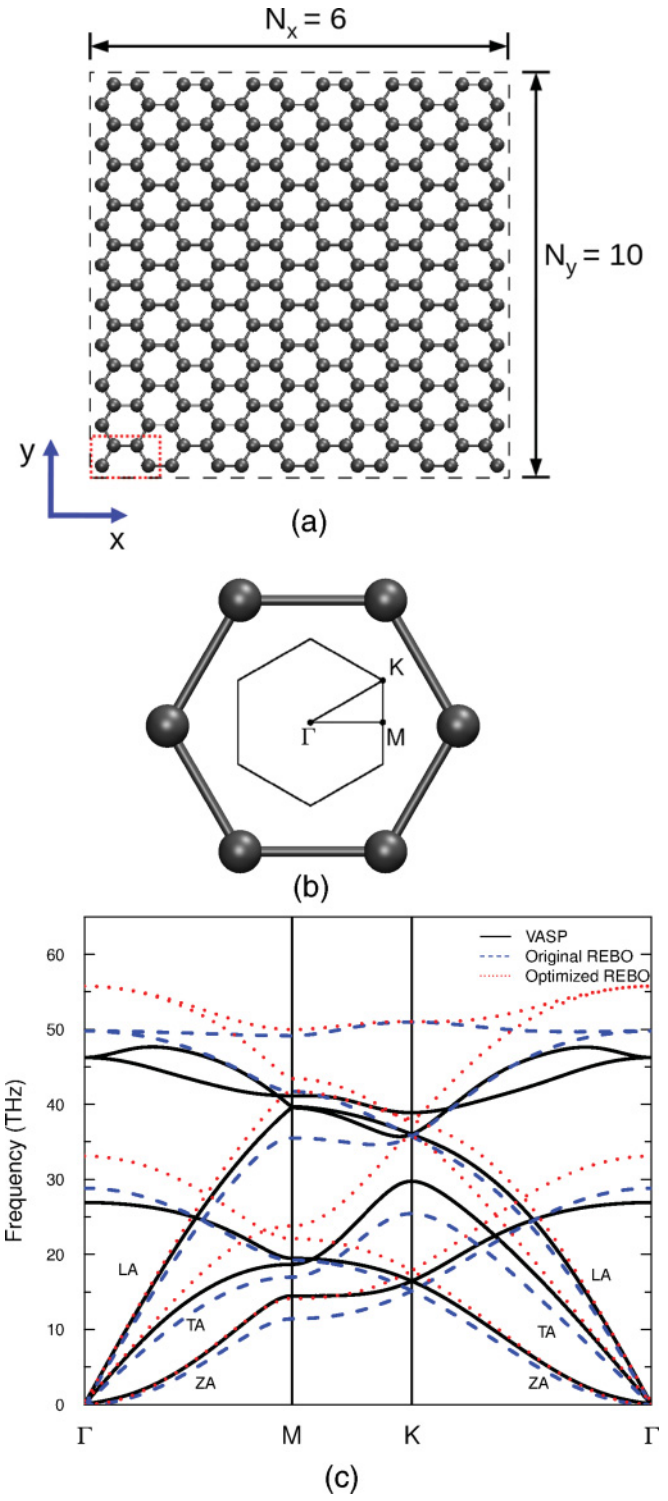

FIG. 1. (Color online) (a) Geometry size of graphene with a periodic boundary condition. The red dotted line enclosed area represents the unit cell, and N_x,N_y denote the number of the repeated unit cell in the x and y directions. The x and y directions also correspond to the armchair and zigzag directions of graphene. The carbon bond length is 1.42 Å. (b) Brillouin zone of graphene and high symmetry points. (c) Phonon dispersions along ΓM, MK, and $K\Gamma$ directions are computed with small displacement methods (Ref.[17]) using force output from DFT, the original REBO, and the optimized REBO. LA and TA represent longitudinal acoustic and transverse acoustic modes, respectively.

correctly model thermal transport in a partially amorphous structure unless it includes a diffusive thermal transport term.[20,21]

B. Green-Kubo method

To compute TC from MD simulations, we use the Green-Kubo method[7,13,16] based on a linear response theory which can express the TC tensor in terms of heat current autocorrelation (HCA), as in the following:

$$\kappa_{xy} = \frac{1}{\Omega K_B T^2} \int_0^\infty \langle J_x J_y \rangle \, d\tau, \tag{1}$$

where Ω is the system volume defined as the area of graphene multiplied with the van der Waals thickness (3.4 Å as used in both theories[4,5] and experiments[1,2]), K_B is the Boltzmann constant, T is the system temperature, and the upper limit of the integral can be approximated by τ_m, which is the correlation time required for HCA to decay to zero ($\tau_m = 0.5$ ns is long enough for HCA to decay to zero). J_x and J_y are denoted as the heat current in the x and y directions, and the angular brackets represent the ensemble average. The exact definition of the heat current and its integration can be found in references.[7,13] The advantage of the Green-Kubo method is that it does not require an artificial thermostat perturbation which may have influence on the heat flux and TC, and the simulation cell size can be small as long as sufficient vibration modes are included for TC to be converged. In addition, the Green-Kubo method can calculate TC in a tensor expression, and then κ_{xx} and κ_{yy} correspond to TC in the x and y directions, respectively. In the following, we first present our microcanonical ensemble (*NVE*) simulation results for isolated pristine graphene at 300 K, and then we investigate the impact of vacancy defects on the TC of graphene.

III. RESULTS AND DISCUSSION

In Fig. 2(a), the TCs of isolated pristine graphene in armchair and zigzag directions, with a periodic boundary (PB) size shown in Fig. 1(a), are computed by averaging the integral of the HCA functions from ten uncorrelated *NVE* ensembles (8 ns for each ensemble). Each sample curve in Fig. 2(a) corresponds to the integral of the HCA function for one *NVE* ensemble, and the averaged sample curve is the average of them. The majority of the sample curves are well converged after $\tau_m = 0.5$ ns. Although some curves show drift behavior due to noise in the HCA,[22] the averaged sample curves are less influenced by the observed drift from particular *NVE* ensembles. The average values and uncertainties of TC can be determined from the averaged sample curves in the region between 0.5 and 0.9 ns for τ_m. It is worth mentioning that the TC value in the y direction of ensemble 4 is negative when τ_m is ~0.8 ns, as shown in the top panel of Fig. 2(a). This temporary unphysical result can be understood by the mode negative correlation effects reported by Henry *et al.*,[16] and a reasonably accurate TC value should be averaged over sufficient number of *NVE* ensembles. In our case, the average TC is converged and is always positive. In Fig. 2(b), we plot a normalized HCA function to show its decay trend for ensembles marked with numbers from 1 to 4 in Fig. 2(a). Ensembles 1 and 3,

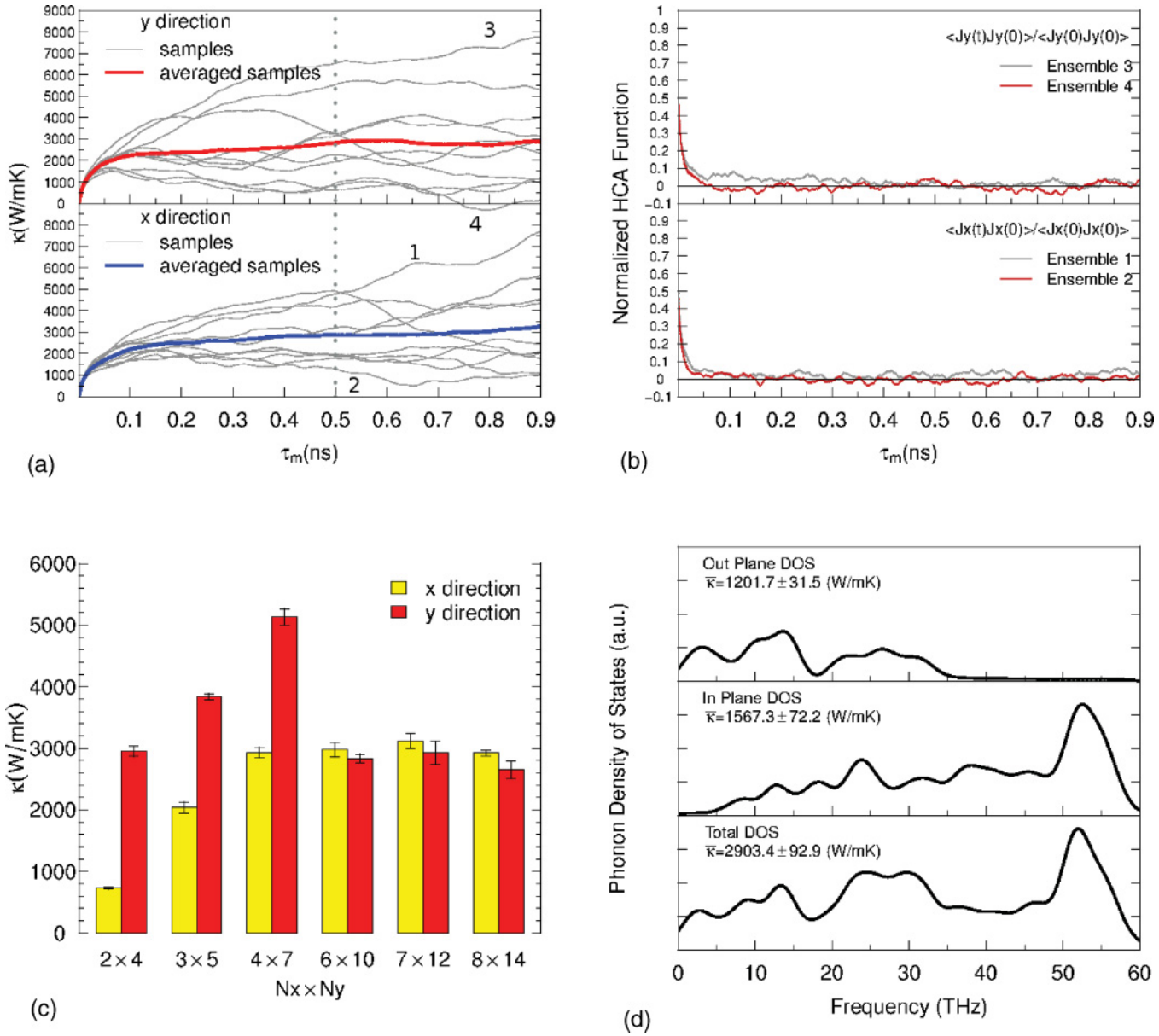

FIG. 2. (Color online) (a) TC of graphene in the x and y directions as a function of τ_m. The solid thin lines (light gray) represent the integral of HCA from ten *NVE* ensembles, and the solid thick lines (red/gray and blue/dark gray) represent the averaged TC values from the integral of HCA of ten *NVE* ensembles. (b) Normalized HCA functions for ensembles marked with numbers from 1 to 4 in (a). (c) TC of graphene in different PB boundary sizes. (d) Phonon DOS analysis in cases of in-plane vibration, out-of-plane vibration, and free vibration.

plotted with gray lines, correspond to the ones that yield the highest TC value, and ensembles 2 and 4, plotted with red (dark) lines, correspond to the ones that yield the lowest TC value. From the HCA function plot, we find that different ensembles may have different HCA function decay rates, and this mainly accounts for the variance of the converged TC value of each *NVE* ensemble. Ideally, the TC value calculated from different *NVE* ensembles should be the same as long as the phase trajectory sampling is sufficient. However, achieving good sampling for each *NVE* ensemble is not practical in that it may require a prohibitively long simulation time. To overcome this difficulty, we can calculate the TC from ten *NVE* ensembles with different initial conditions so as to expand the phase trajectory sampling, and then average them to obtain a converged and reliable TC value. We also test the PB size effect on the TC of graphene. In Fig. 2(c), the gradually increased and finally converged TC can be explained by the PB cutoff effect on the phonon wavelength.[23] As the PB size increases, more long-wavelength phonon modes, which are dominant heat-carrying modes, can be excited and contribute to heat transport. However, adding even more long-wavelength modes may also strengthen phonon scattering so that the TC will not diverge. For computational efficiency, we choose a PB size of 6×10 in the following simulations. Figure 2(c) also suggests that heat transport along the zigzag and armchair directions in graphene is isotropic, and this feature is different from the

anisotropic results for a graphene nanoribbon in that irregular chiral angle edges in the graphene nanoribbon can have a stronger scattering effect.[6,24]

We further investigate which polarization mode (i.e., ZA or LA and/or TA acoustic modes) may account for the superior TC of isolated pristine graphene. This was once reported in previous BTE calculations,[4,5] and there is disagreement on whether the ZA modes are the majority phonon heat carriers. Here, we try to address this controversy through MD simulations. By freezing certain degrees of freedom of atomic motion, we can restrict atomic motion into in-plane vibration and out-of-plane vibration cases. This freezing method can therefore decouple the phonon scattering interaction between in-plane and out-of-plane phonons. Then, the TC of graphene from the in-plane and out-of-plane contributions can be determined from *NVE* simulations, as shown in Fig. 2(d). The validity of the freezing method relies on the strength of the scattering interaction between the in-plane and out-of-plane phonons. If the interaction is weak, the freezing method can give a reasonable approximation to estimate the contribution of the ZA phonons to the total TC. Otherwise, there is no guarantee that the result is valid and accurate. In fact, we may use the freezing method to diagnose whether the in-plane and out-of-plane phonons in graphene have a strong interaction. If there is a strong interaction, as we use the freezing method to decouple the interaction, in-plane LA and/or TA phonons are less scattered by out-of-plane phonons, and the in-plane vibration case would give a higher TC. Similarly, out-of-plane ZA phonons are less scattered by in-plane phonons, and the out-of-plane vibration case would also give a higher TC. Then, the addition of the two parts should be apparently larger than the total TC in the strong interaction case. However, if it is a weak interaction case, the addition of the two parts (2769 W/mK) should not be larger than the total TC (2903 W/mK), which is what we observed from the simulation. Therefore, in the weak interaction case, the freezing method can quantitatively estimate that the out-of-plane acoustic modes (i.e., ZA) contribute ∼43% of the total TC. In Fig. 2(d), we also calculate the phonon DOS by performaing a fast Fourier transform of the velocity autocorrelation function,[25,26] and a Gaussian smearing width of 1.5 THz is applied to smooth the spikes in the phonon DOS. From the comparison between the in-plane and out-of-plane DOS, the large amount of ZA states at a frequency lower than 5 THz may explain that those ZA modes can also have a large contribution to the TC even if their group velocities are much smaller as compared to those of the LA and/or TA modes. Identifying such a large contribution from the ZA modes would help to understand why the graphene TC may be largely reduced when it makes contact with a substrate in a recent experiment.[3]

We now concentrate on the impact of vacancy defects on the TC of graphene. In practice, depending on the synthesis procedure and observation method, or a particular irradiation method to artificially modify its properties,[27–29] graphene would inevitably have complex defects, such as single vacancies,[10] Stone-Wales defects,[30] grain boundaries,[31] and reconstructed defect structures.[32] Here, we do not investigate them all but mainly focus on single vacancies, which have been recently identified as major defects in experiment.[10] Thus, we generate vacancy sites through randomly removing a given number of carbon atoms from the structure shown in Fig. 1(a). We find that even for a very low vacancy concentration ∼0.42% (i.e., one of 240 atoms removed), TC reduction can be significant, as shown in Fig. 3(a) (e.g., 118.10 W/mK). As the vacancy sites increase to 8.75% (i.e., 21 of 240 atoms removed), the TC can be reduced to 3.08 ± 0.31 W/mK. It is the obvious *D* peak from the Raman spectrum that leads us to speculate that there might be such a high vacancy concentration for chemically reduced graphene oxide,[11] and our simulation result shows that a dramatic TC reduction occurs below ∼3% vacancies, and the reduction trend turns out to be slow for higher concentrations. In Fig. 3(a), we also check the PB size effect for a 8×14 simulation box with the same vacancy concentration. A comparison of the results found for small and large simulation boxes suggests that a 6×10 simulation box is still able to have sufficient phonon modes to accurately describe the phonon scattering interaction with vacancy defects. To understand more clearly the TC reduction trend, in the top panel of Fig. 3(b) we plot phonon DOS evolution as the vacancy sites increase. From the DOS figure, there are mainly two factors that can cause

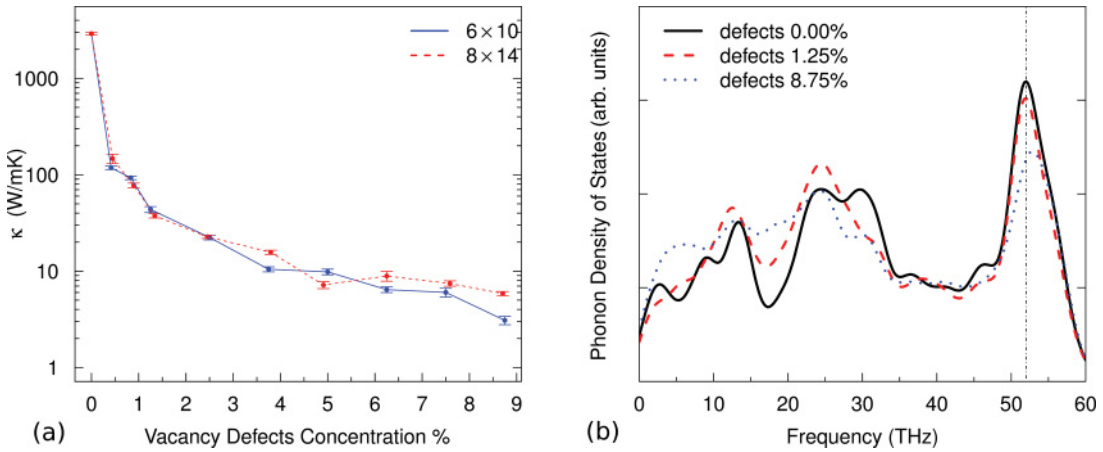

FIG. 3. (Color online) (a) TC of graphene as a function of vacancy defect concentration. The solid blue (dark gray) line and the dashed red (gray) line correspond to PB sizes of 6×10 and 8×14, respectively (b) Phonon DOS analysis on the effect of vacancy defects.

an abrupt TC reduction. The first one is the broadening of the phonon mode peaks around phonon modes of 15 THz, where the valley-shaped curves are almost flattened by the broadening of nearby peaks as the vacancy concentration increases. The broadening of the phonon modes indicates a reduction of the lifetime of the corresponding modes. Therefore, the mean free path of those modes as well as their contribution to the total TC are reduced. The second factor is an average increase of DOS value below 15 THz. In the following equation,

$$\frac{1}{\tau_p} = C\left(\frac{\Delta M}{M}\right)^2 \frac{\pi\omega^2 g(\omega)}{2G}, \tag{2}$$

Klemens has shown that relaxation time τ_p due to point defect scattering is inverse proportional to both the vacancy concentration C and the DOS value $g(\omega)$.[33] So average increase of DOS for low-frequency modes may also cause a further reduction in the relaxation time and mean free path. Apart from the above observed features, a slight blueshift for high-frequency optical modes is also identified. As the bonds near the vacancy sites in principle would be stiffer due to the loss of coordination (i.e., bond stiffness gets closer to a double or triple bond), this should account for the observed blueshift.

IV. CONCLUSIONS

In this paper, we have investigated phonon transport in graphene at 300 K with an optimized REBO carbon potential to accurately predict the TC of isolated pristine graphene as well as one with vacancy defects. We show that the TC of isolated pristine graphene (e.g., ~2900 W/mK) agrees well with both BTE theories and experiments, and the ZA mode makes a sizable contribution to the large TC of graphene. We also find that an extremely low TC at 300 K (e.g., ~3 W/mK) is possible to achieve when graphene has 8.25% vacancy defects. Our simulation results have shown the significant impact of vacancy defects on the TC of graphene.

ACKNOWLEDGMENTS

The authors acknowledge support from SWAN.

*kjcho@utdallas.edu

[1] S. Ghosh, I. Calizo, D. Teweldebrhan, E. P. Pokatilov, D. L. Nika, A. A. Balandin, W. Bao, F. Miao, and C. N. Lau, Appl. Phys. Lett. **92**, 151911 (2008).
[2] W. Cai, A. L. Moore, Y. Zhu, X. Li, S. Chen, L. Shi, and R. S. Ruoff, Nano Lett. **10**, 1645 (2010).
[3] J. H. Seol, I. Jo, A. L. Moore, L. Lindsay, Z. H. Aitken, M. T. Pettes, X. Li, Z. Yao, R. Huang, D. Broido, N. Mingo, R. S. Ruoff, and L. Shi, Science **328**, 213 (2010).
[4] D. L. Nika, E. P. Pokatilov, A. S. Askerov, and A. A. Balandin, Phys. Rev. B **79**, 155413 (2009).
[5] L. Lindsay, D. A. Broido, and N. Mingo, Phys. Rev. B **82**, 115427 (2010).
[6] W. J. Evans, L. Hu, and P. Keblinski, Appl. Phys. Lett. **96**, 203112 (2010).
[7] H. Zhang, G. Lee, A. F. Fonseca, T. L. Borders, and K. Cho, J. Nanomater. **2010**, 537657 (2010).
[8] A. A. Balandin, S. Ghosh, W. Bao, I. Calizo, D. Teweldebrhan, F. Miao, and C. N. Lau, Nano Lett. **8**, 902 (2008).
[9] D. Konatham and A. Striolo, Appl. Phys. Lett. **95**, 163105 (2009).
[10] M. H. Gass, U. Bangert, A. L. Bleloch, P. Wang, R. R. Nair, and A. K. Geim, Nat. Nanotech. **3**, 676 (2008).
[11] W. Gao, L. B. Alemany, L. Ci, and P. M. Ajayan, Nat. Chem. **1**, 403 (2009).
[12] L. Lindsay and D. A. Broido, Phys. Rev. B **81**, 205441 (2010).
[13] P. K. Schelling, S. R. Phillpot, and P. Keblinski, Phys. Rev. B **65**, 144306 (2002).
[14] H. C. Schniepp, J. Li, M. J. McAllister, H. Sai, M. H. Alonso, D. H. Adamson, R. K. Prud'homme, R. Car, D. A. Saville, and I. A. Aksay, J. Phys. Chem. B **110**, 8535 (2006).
[15] J. Che, T. Cagin, and W. A. Goddard III, Nanotechnology **11**, 65 (2000).
[16] A. Henry and G. Chen, Phys. Rev. B **79**, 144305 (2009).
[17] Dario Alfè, program available at [http://www.homepages.ucl.ac.uk/~ucfbdxa/phon] (1998).
[18] We use the Vienna *ab initio* simulation package (VASP) to compute forces induced by displaced atoms in graphene with projected augmented-wave pseudopotentials in a generalized gradient approximation. Then, we use code (Ref. 17) to compute the phonon dispersion of graphene with a small displacement method. The energy cutoff of the plane-wave basis is 400 eV, and a distance of 10 Å is used to minimize the graphene interaction with its periodic images.
[19] D. W. Brenner, O. A. Shenderova, J. A. Harrison, S. J. Stuart, B. Ni, and S. B. Sinnott, J. Phys. Condens. Matter **14**, 783 (2002).
[20] D. Donadio and G. Galli, Phys. Rev. Lett. **102**, 195901 (2009).
[21] Y. He, D. Donadio, J. Lee, J. C. Grossman, and G. Galli, ACS Nano **5**, 1839 (2011).
[22] D. P. Sellan, E. S. Landry, J. E. Turney, A. J. H. McGaughey, and C. H. Amon, Phys. Rev. B **81**, 214305 (2010).
[23] D. Donadio and G. Galli, Phys. Rev. Lett. **99**, 255502 (2007).
[24] J. Hu, X. Ruan, and Y. P. Chen, Nano Lett. **9**, 2730 (2009).
[25] J. M. Dickey and A. Paskin, Phys. Rev. **188**, 1407 (1969).
[26] M. P. Allen and D. J. Tildesley, *Computer Simulation of Liquids* (Oxford University Press, New York, 1987).
[27] M. M. Ugeda, I. Brihuega, F. Guinea, and J. M. Gómez-Rodríguez, Phys. Rev. Lett. **104**, 096804 (2010).
[28] A. V. Krasheninnikov and F. Banhart, Nat. Mater. **6**, 723 (2007).
[29] K. Carva, B. Sanyal, J. Fransson, and O. Eriksson, Phys. Rev. B **81**, 245405 (2010).
[30] J. Ma, D. Alfè, A. Michaelides, and E. Wang, Phys. Rev. B **80**, 033407 (2009).
[31] Y. Liu and B. I. Yakobson, Nano Lett. **10**, 2178 (2010).
[32] G. D. Lee, C. Z. Wang, E. Yoon, N. M. Hwang, D. Y. Kim, and K. M. Ho, Phys. Rev. Lett. **95**, 205501 (2005).
[33] P. G. Klemens and D. F. Pedraza, Carbon **32**, 735 (1994).